CO_2 reactivity of briquettes derived from discard inertinite-rich Highveld coal using lignosulphonate and resin as binders

N.T. Leokaoke[1], J.R. Bunt[1], H.W.J.P. Neomagus[1], F.B. Waanders[1], and C.A. Strydom[2]

Affiliation:
[1]School of Chemical and Minerals Engineering, Research Unit for Energy and Technology Systems, North-West University, Potchefstroom Campus, South Africa.
[2]Chemical Resource Beneficiation (CRB), North-West University, Potchefstroom Campus, South Africa.

Correspondence to:
N.T. Leokaoke

Email:
Nthabiseng.Leokaoke@nwu.ac.za

Dates:
Received: 18 Apr. 2019
Revised: 11 Jun. 2019
Accepted: 12 Jun. 2019
Published: October 2019

How to cite:
Leokaoke, N.T., Bunt, J.R., Neomagus, H.W.J.P., Waanders, F.B., and Strydom, C.A. CO_2 reactivity of briquettes derived from discard inertinite-rich Highveld coal using lignosulphonate and resin as binders.
The Southern African Insitute of Mining and Metallurgy

DOI ID:
http://dx.doi.org/10.17159/2411-9717/720/2019

Synopsis

South African collieries generate approximately 31 Mt of fine and ultrafine coal annually, with the majority of the ultrafine fraction discarded in slurry ponds and underground workings. Use can be made of this energy source through briquetting, thereby alleviating the handling problems associated with fine coal. Briquettes of inertinite-rich high-ash coal when combined lignosulphonate and resin have shown promising mechanical strength, therefore requiring reactivity analysis. In this study, chars derived from lump coal, binderless briquettes, and lignosulphonate- and resin-bound briquettes were subjected to CO_2 gasification at 875, 900, 925, 950, and 1000°C. Binder addition brought about no distinct difference in char reactivity. The briquetted chars showed approximately double the reactivity of lump coal chars. The increase in micropore surface area derived during the devolatilization process is postulated to be the major contributor to the increased reactivity of the briquettes. No significant differences were observed between the activation energy of the lump coal and manufactured briquettes, with values ranging between 222–229 kJ/mole. Industrial implementation of fine coal briquetting in South Africa will result not only in an increase in coal resources, but also reduce environmental concerns linked to fine coal discards.

Keywords
CO_2 gasification, reactivity, discard coal, kinetics, briquetting, porosity.

Introduction

About 12% of South African run-of-mine (ROM) coal is classified as fine (–0.5 mm) and ultrafine (–0.1 mm), with the majority of the ultrafine fraction being discarded into slimes dams and underground workings as a result of handling, transportation, and utilization limitations (England, 2000; Mangena and du Cann, 2007). Bell *et al.* (2001) reported sulphur contents of up to 3.8% for discard coals from the Witbank coalfields. One of the major environmental risks associated with sulphide minerals in discard coals is acid rock drainage (Kotsiopoulos and Harrison, 2017). Industrial utilization of fine coal tailings can alleviate the environmental hazards associated with disposal, while increasing the coal resources in fossil fuel-dependent countries such as South Africa. A study by Wagner (2008) indicated that typical discard coal aged up to 40 years can contain between 18 and 40% mineral matter, with the lowest fixed carbon content determined as 37% (d.b.). The finer fraction (1.18 mm) had heating values as high as 21 MJ/kg (a.d.), and can therefore be classified as a viable source of energy (Wagner, 2008).

For local applications, fine discard coal can be briquetted for use in technologies that require lump coal, such as fixed-bed gasifiers. For large-scale application, briquettes can be utilized in the fixed-bed dry bottom (FBDB) gasification technology, which accounts for the conversion of over 30 Mt of coal into liquid fuels annually in South Africa (van Dyk, Keyser, and Coertzen, 2006). The FBDB gasifier is designed to accommodate a variety of carbonaceous materials with ash and moisture contents up to 35% and 30%, respectively. Although the FBDB gasifier is designed for a top particle size of 70 mm and a bottom size of 5–8 mm, a study conducted by Bunt and Waanders (2008) showed that the most stable thermal particle size in the gasifier is between 6.3 and 25 mm (van Dyk, Keyser, and Coertzen, 2006; Bunt and Waanders, 2008).

Briquettes, like ROM coal, are expected to be mechanically strong, water resistant, thermally stable, and reactive (Richards, 1990; Mangena *et al.*, 2004; Bunt *et al.*, 2015). During briquette formation, the reactive macerals break and subsequently link into joint masses at the briquette surface. This

phenomenon, less prevalent during briquetting of inertinite-rich fine coal, is responsible for the increased mechanical strength of vitrinite-rich coal briquettes. Leokaoke *et al.*, (2018) concluded that the addition of lignosulphonate and resin as binders increased the mechanical strength of briquettes derived from inertinite-rich Highveld coal fines. Above 5 wt% lignosulphonate addition, the cured briquettes surpassed the compressive strength of ROM coal from the same colliery. At 10 wt% resin addition, the cured briquettes could withstand a compressive force of 12 MPa. Water resistance analysis of the inertinite-rich, low grade coals investigated by Leokaoke *et al.* (2018), Mangena *et al.* (2004), and Mangena and du Cann (2007) resulted either in the disintegration of the briquettes in water or reduced wet strengths. This was ascribed to the kaolinite mineral matter in conjunction with high ash content (> 15 wt%) plasticizing in the presence of excess water (Mangena and du Cann, 2007). Applying a molten wax and paraffin coating to the surfaces of the briquettes after curing rendered the lignosulphonate- and resin-bound briquettes water resistant (Leokaoke *et al.*, 2018).

As regards the thermal characteristics of briquettes, properties such as moisture content, calorific value, emissions, and heat retention during combustion, as well as gasification reactivity have been studied (Rubio, Izquierdo, and Segura, 1999; Mishra, Sharma, and Agarwal, 2000; Tarasov, Shahi, and Leitch, 2013; Massaro, Son, and Groven, 2014; Bunt *et al.*, 2015). The agglomerates produced should contain less than 30% moisture to be suitable for FBDB gasification (van Dyk,Keyser, and Coertzen, 2006). The additives used are expected to not significantly reduce, if not enhance, the calorific value of the raw coal (Rubio, Izquierdo, and Segura, 1999; Mishram Sharma, and Agarwal, 2000). While investigating the rate of conversion of manufactured binderless briquettes and ROM coal, Bunt *et al.* (2015) established that briquetted chars reached complete conversion faster than ROM coal char of similar size. Although the briquetting process proved to enhance reactivity, the effect of binder addition on briquette reactivity still requires investigation.

The majority of South African coalfields consist of inertinite-rich coal. In this study the aim is to analyse the reactivity of briquettes derived from South African inertinite-rich, low-grade coal fines. The reactivity of briquettes manufactured using lignosulphonate and resin as binders is compared to that of ROM coal. The study is concluded with the description of a kinetic model to predict CO_2 gasification rates for the manufactured briquettes and ROM coal.

Experimental procedure

Coal

The medium rank C, low-grade, inertinite-rich filter cake discard coal was obtained from an active colliery in the Highveld area, South Africa. The sample contained 20 wt% surface moisture as received, with a d_{80} of 100 µm. ROM coal from the same colliery was obtained for comparison. The standard characterization techniques used were petrographic, proximate, total sulphur, ultimate, and XRF analyses as indicated in Table I and Table II.

The petrographic analyses (Table I) indicate that the ROM coal is inertinite-rich. XRF analyses for both the coal fines and ROM coal are presented in Table II. The mineral matter in both the coal and coal fines mostly comprised Si-, Al-, and Ca-containing species. An alkali index (AI), as proposed by Sakawa, Sakurai, and Hara (1982), was determined for both the ROM and coal fines by means of Equation [1], and can be seen in Table II.

Table I

Coal properties

	Coal fines	ROM coal
Proximate analysis (wt%, db[a])		
Ash	24.3	19.8
Volatile matter	27.7	24.1
Fixed carbon	48.1	56.0
Ultimate analysis (wt%, dafb[b])		
Carbon	79.2	78.6
Hydrogen	4.8	4.0
Nitrogen	2.2	2.1
Oxygen	12.6	14.7
Sulphur	1.2	0.6
Gross calorific value (MJ/kg, adb[c])		
	22.3	26.0
ROM coal petrographic analysis (vol.%, mmb[d])		
Vitrinite		27.7
Liptinite		5.4
Inertinite		56.1
Visible minerals		10.8
Total reactive macerals (vol%)		63.8
Reflectance properties (%)		
Mean vitrinite random reflectance (Rr)		0.65
Rank		Bituminous medium rank C

[a]db – dry basis, [b]dafb – dry, ash-free basis, [c]adb – air-dried basis, [d]mmb – mineral matter basis

Table II

XRF analysis (ASTM D4326) for the coal fines and ROM coal ash

	Coal fines (wt%, LOIfb*)	ROM coal (wt%, LOIfb)
SiO_2	47.9	50.1
Al_2O_3	26.4	24.4
CaO	7.4	10.7
SO_3	6.2	5.6
Fe_2O_3	5.0	1.8
MgO	2.4	3.3
TiO_2	1.4	1.3
K_2O	1.1	0.6
P_2O_5	0.8	0.6
Na_2O	0.4	0.8
SrO	0.4	0.4
BaO	0.3	0.2
MnO	0.1	0.1
ZrO_2	0.1	0.1
Alkali Index (-)	**5.3**	**4.6**

* Loss on ignition free basis

$$AI = \frac{CaO + Fe_2O_3 + MgO + K_2O + Na_2O}{SiO_2 + Al_2O_3} \times ash\% \quad [1]$$

The concentrations of the organic species identified in the samples are typical for South African Highveld coal (van Dyk, Keyser, and Coertzen, 2009; Matjie *et al.*, 2011).

Additives

The lignosulphonate utilized was a paper-pulp by-product from the paper industry in South Africa. The proximate and ultimate analyses of the lignosulphonate are shown in Table III.

Table III

Binder properties

	Lignosulphonate	Resin
Proximate analysis (wt%, db*)		
Ash content	17.6	0.9
Volatile matter	79.3	95.2
Fixed carbon	3.1	4.0
Gross calorific value (MJ/kg, adb†)		
15.1	31.5	

*db – dry basis, †adb – air-dried basis

Prior to utilization, the lignosulphonate was milled in a ball mill to –1 mm. The resin obtained was a NCS 991 PA MV polyester resin with average density and viscosity (at 25°C) of 1.11 g/cm³ and 495 mPa.s, respectively. The resin required no pre-treatment prior to addition to the coal fines.

Briquetting process

The briquettes were produced in a 13 x 13 mm cylindrical die, using a Lloyd LRX Plus press. While investigating the effect of different binders on mechanical strength, Leokaoke *et al.* (2018) showed that the addition of lignosulphonate and resin at 5 and 7.5 wt% respectively increased the briquette compressive strength to approximately that of the ROM coal analysed (14 MPa), comparing well with briquettes prepared in previous studies (Mangena and du Cann, 2007; Teixeira, Pena, and Miguel, 2010; Bunt *et al.*, 2015). The coal fines investigated in this study were of the same origin, therefore lignosulphonate and resin were each added in weight concentrations of 5.0 and 7.5%. Samples of 2.5 g were prepared and pressed with a force of 4.0 kN. Optimum curing conditions were previously found to be 100°C and 3 hours for binderless briquettes (Leokaoke *et al.*, 2018). These curing conditions were subsequently utilized for briquettes prepared both with and without binders. For comparison, cylindrical samples of the ROM coal were prepared by means of shaping lump coal to dimensions of 13 x 13 mm using a grinder and metal file. Samples with a weight of 2 ± 0.3 g were selected for analysis. The samples were stored in an oven maintained at 105°C.

Porosimetry

The porosity and surface area of the coal briquettes and ROM coal were analysed by means of CO_2 adsorption on a Micromeritics ASAP 2020 surface area and porosity analyser. Samples of approximately 0.35 g were prepared through breakage of the cylindrical briquettes and ROM coal and were subsequently degassed at 75°C at a vacuum pressure of 300 µm Hg for 24 hours. Upon completion, the sample micropore surface area was analysed with CO_2 at 0°C using an ice bath. The micropore surface area was determined with the Brunauer-Emmet-Teller (BET) and Dubinin-Radushkevich (D-R) methods. The maximum micropore volume and median diameter were determined using the CO_2 adsorption Horvath-Kawazoe (H-K) method. The sample porosity was calculated by evaluating the area beneath the D-R cumulative pore volume plot (Okolo *et al.*, 2015).

The skeletal (helium) densities were analysed using a Micromeritics Accupyc II 1340 gas pycnometer consisting of a 10 cm³ sample cell and expansion chamber. The sample cell was filled to approximately 75 vol.% (three briquettes). The cell was pressurized with helium which was allowed to expand into the expansion chamber, providing two pressure readings per sample. The recorded pressures were converted to sample volume and used in conjunction with the known sample mass to determine the sample density (Huang *et al.*, 1995).

The particle (mercury) densities were determined by means of mercury submersion. The set-up was placed inside a ventilation chamber and consisted of a Sartorius ED 4202S balance, a cell containing mercury with purity greater than 99.5%, and a particle plunger. Single particles were used per measurement. The cell was placed on the balance and the briquette and plunger were submerged into the mercury (separately and combined). The weights recorded were converted to density using Archimedes' principle (Coetzee *et al.*, 2014).

Reactivity

Thermal fragmentation testing was conducted in an Elite Thermal Systems Ltd tube furnace model TMH16/75/610. The furnace was preheated to 100°C prior to inserting the briquettes and ROM coal. After inserting the sample, the furnace was heated to 700°C at a rate of 5°C/min with a hold time of 1 hour prior to cooling to room temperature. The thermal fragmentation analysis was completed under nitrogen gas of purity greater than 99.99% (Afrox South Africa), at a flow rate of 5 NL/min.

The devolatilization and gasification of the coal were executed separately. Devolatilization was performed in the Elite tube furnace model TMH16/75/610. Upon inserting the coal, the furnace was heated at 5°C/min to 1000°C with a hold time of 15 minutes under nitrogen gas at a flow rate of 5 NL/min.

Gasification of the coal was performed in an in-house-manufactured, large particle thermogravimetric analyser (TGA) as described by Coetzee *et al.* (2013). The TGA consists of a Lenton-supplied, vertical Elite Thermal Systems Ltd furnace model TSV 15/50/180. The sample was loaded into a quartz bucket, which was placed on top of a Radwag precision PS 750/C/2 mass balance. The furnace was equipped with a K-type thermocouple to measure the temperature in the reaction zone. The sample holder was inserted into the predetermined reaction zone of the furnace and isothermal gasification reactions were conducted at 875, 900, 925, 950, and 1000°C. Afrox supplied CO_2 gas (with a purity of 99.99%), which was fed at 2 NL/min for the duration of the gasification experiments using a Brooks model 0254 mass flow controller. Gasification experiments were considered complete when no further mass loss was observed.

The mass loss of the sample with time, as well as the reaction temperatures, was logged and saved. A polynomial curve in the form of Equation [2] (nomenclature provided at the end of the paper) was subsequently fitted to the logged mass loss data using the sum of the least squares method in order to filter the data.

$$m_t = a_n t^n + a_{n-1} t^{n-1} + \ldots + a_1 t + a_0 \quad [2]$$

The conversion was then determined by (Coetzee *et al.*, 2013):

$$X = \frac{m_i - m_t}{m_i - m_{ash}} \quad [3]$$

The conversion rate was determined as:

$$\frac{dX}{dt} = -\frac{[n a_n t^{n-1} + (n-1) a_{n-1} t^{n-2} + \ldots + a_1]}{m_i - m_{ash}} \quad [4]$$

Results and discussion

During thermal fragmentation analysis, the briquettes all maintained their shape and size, merely showing cracks at the particle surfaces as indicated for lignosulphonate-bound briquettes in Figure 1. Similar observations were made for binderless and resin-bound briquettes. This is in agreement with the findings of Bunt and Waanders (2008), who concluded that Highveld coal particles smaller than 25 mm are not prone to fragmentation during the fixed bed gasification process.

Porosimetry

In Figure 2a the skeletal and particle densities of the charred and uncharred briquettes as well as ROM coal are shown (average values indicated). The CO_2 micropore surface area data, consisting of the BET and D-R micropore surface area, H-K maximum pore volume and porosity, with the standard deviation, are reported in Figure 2b. Prior to charring, the ROM coal exhibited higher micropore surface area than the manufactured briquettes. This trend was also observed in the briquette and ROM coal porosities and can be attributed to the physical packing of fines during the briquetting process, reducing pore accessibility by the adsorbate. No significant differences were observed between median pore diameters of the briquettes and the ROM coal (with their respective chars), with a median pore diameter of 3.96 ± 0.15 Å. The addition of lignosulphonate and resin reduced the maximum pore volume of the binderless briquettes (BL) by approximately half. This may be a result of the blocking of pores by the added binders (Rubio, Izquierdo, and Segura, 1999). Upon charring, the micropore surface area of the ROM coal reduced from 100 m^2/g to 80 m^2/g. This reduction can be ascribed to the ordering of the carbon structure, reducing the microporosity and subsequently the micropore surface area of the coal particles (Cai *et al.*, 1996; Lu *et al.*, 2002). In contrast to the ROM coal, the manufactured briquettes showed an increase in micropore surface area subsequent to charring. This could be ascribed to the evaporation of binders along with the evolution of micropores during the diffusion of the volatiles formed as a result of the pyrolysis process (Liu, Cao, and Liu, 2015). The D-R micropore surface area of the briquetted chars was found to be in the range of 184 ± 5 m^2/g. The porosity of the briquette and the ROM coal derived chars showed a similar trend to the BET and D-R char micropore surface area. The ROM coal porosity, on the other hand, reduced following charring. The maximum pore volumes of briquetted and ROM coal chars showed a trend similar to porosity. The effect of binder addition was not visible after briquette devolatilization, indicative of binder decomposition during the charring process.

Effect of temperature

The conversion rates of the ROM coal char, binderless (BL), lignosulphonate (L), and resin (R) briquetted chars as a function of carbon conversion are presented in Figure 3. A decrease in the conversion rate was observed as the carbon conversion increased, with the maximum reactivity observed at X = 0. This is related to the size of the briquette, which is much larger than the pulverized coal char samples generally used for kinetic studies, where a maximum reactivity is often observed at X > 0. The absence of a maximum in reactivity compares well to conversion

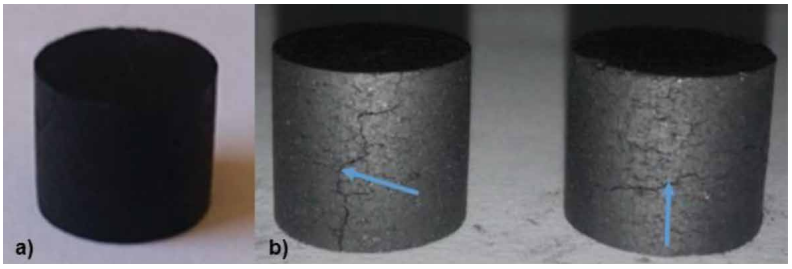

Figure 1—Lignosulphonate-bound briquettes before (a) and after (b) thermal fragmentation

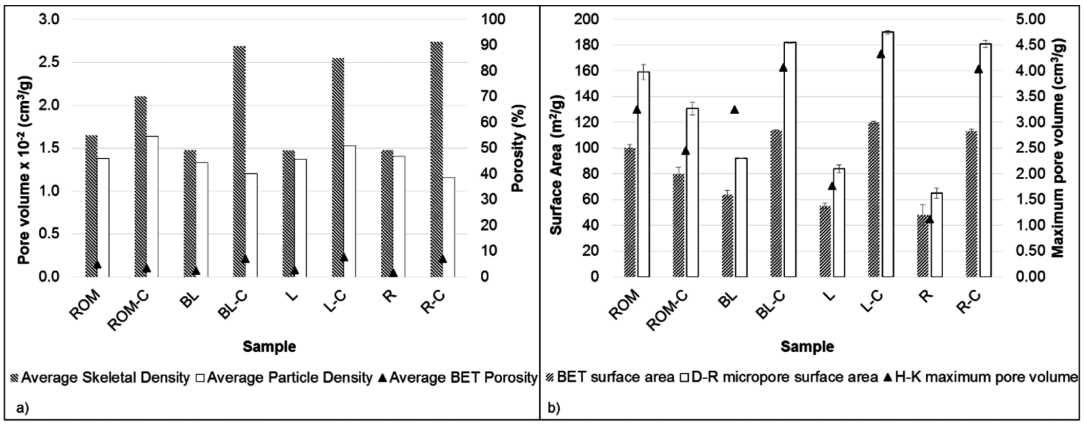

Figure 2—Properties of coal/char from (a) CO_2 gas adsorption, and (b) helium pycnometry and mercury submersion, with ROM – ROM coal, ROM-C – ROM coal char, BL – binderless briquette, BL-C – binderless briquette char, L – lignosulphonate briquette, L-C – lignosulphonate briquette char, R – resin briquette, R-C – resin briquette char

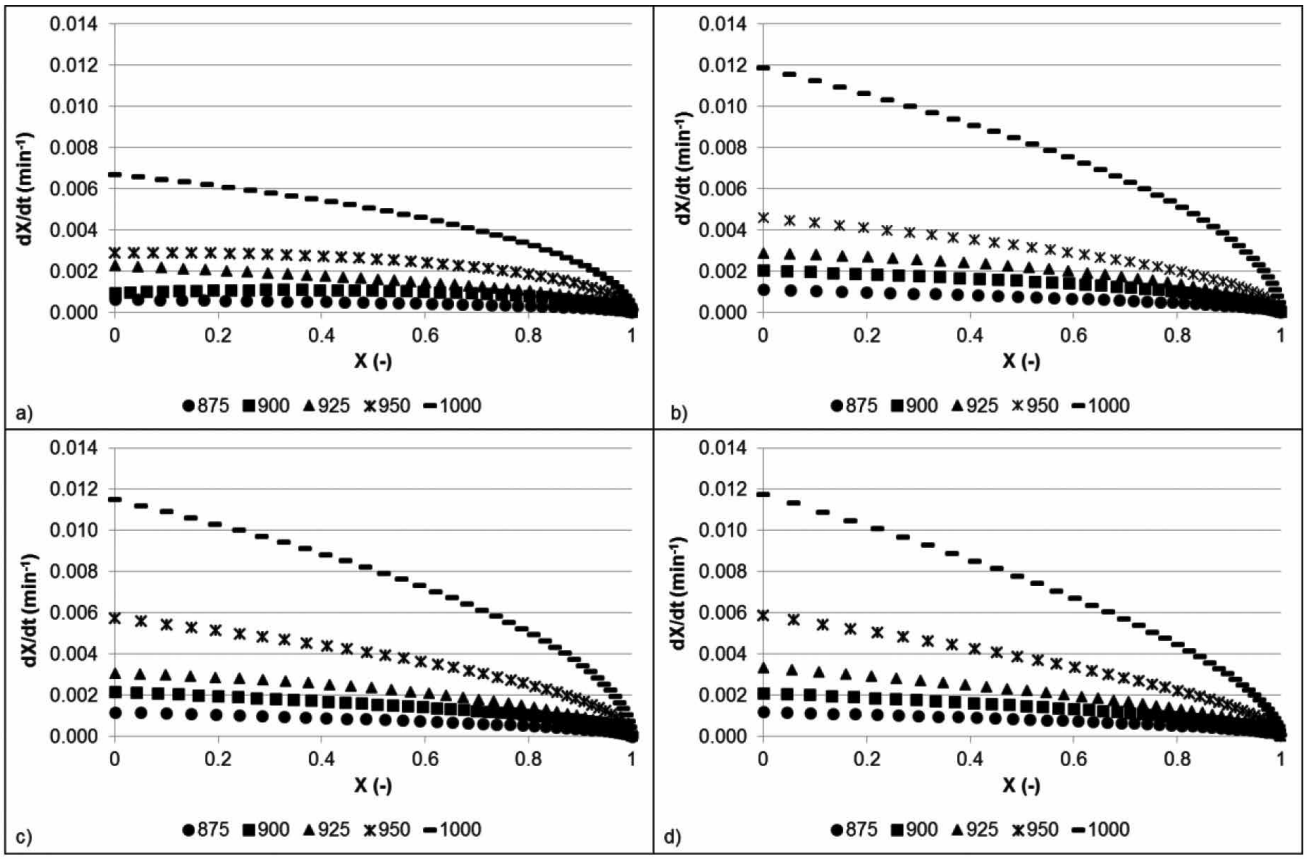

Figure 3—Conversion rates of (a) ROM coal char, (b) BL, (c) L, and (d) R briquette chars

curves obtained for lump coal particles, as shown by Coetzee *et al.* (2013). Catalytic influences were considered to be negligible, which can be attributed to the low concentration of catalytic metals, such as CaO and K_2O, in the mineral matter for both the ROM coal and coal fines, as seen from the XRF analysis in Table II (Ochoa *et al.*, 2001; Kucherenko *et al.*, 2010; Coetzee *et al.*, 2013). Elevation of the reaction temperature led to an increase in the initial reactivity for the coals.

Effect of binder addition

The effect of binder addition on the conversion rate at temperatures between 875 and 1000°C is presented in Figure 4. No significant difference between the reactivity of the BL, L, and R briquetted chars was observed at the five reaction temperatures. Brebu, Cazacu, and Chirila (2011) determined that lignosulphonate disintegrates between 140 and 550°C, hence no significant influence in reactivity was observed subsequent to the charring process. The boiling point of polyester resin is in the range of 145–148°C and resin is thus also evaporated during the charring process. The addition of the two binders contributed solely to the mechanical strength of the briquettes and had no effect on briquette reactivity. The differences in CO_2 micropore surface areas of the briquettes were also more pronounced prior to charring. Briquetted chars exhibited D-R surface areas between 181 and 190 m^2/g, while the ROM coal char exhibited a lower D-R micropore surface area of 131 m^2/g. This is evident from the difference in char reactivity of the ROM coal and briquettes. Bunt *et al.*, (2015) observed similar trends between briquette and ROM coal char reactivity. Similarly, the porosities of the BL, L, and R briquette chars were higher than for the ROM coal char, again substantiating the observed CO_2 char reactivities. During analysis of pore evolution, Liu, Cao, and Liu (2015) found that pore evolution had a great influence on micropore surface area, and in turn, gasification reaction rate.

Kinetic modelling

The reactivity results were modelled using the Wen model. The semi-empirical model was developed for a wider variety of pore structure evolution as a result of carbon conversion. This was achieved by introducing a second variable, the reaction order (m), as seen in Equation [5] (Wen, 1968):

$$\frac{dX}{dt} = k(1-X)^m \quad [5]$$

The Wen model reactivity predictions, compared to the experimental data) at 875°C, are given in Figure 5. The model described the CO_2 gasification rate well for the cylindrical particles, with an average minimum quality of fit (QOF) of 89%, as indicated in Table IV.

Table IV shows the reaction order and reactivity constant values predicted using the Wen model. The reaction order showed no definitive trend with increasing temperature. An average value of 0.48 was obtained for the gasification experiments, which is similar to the assumed 0.5 for cylindrical particles when applying the shrinking unreacted core model (SUCM) in the chemical reaction-controlled regime (Mahinpey and Gomez, 2016). The reaction order was generally found to be lower for ROM coal than

CO_2 reactivity of briquettes derived from discard inertinite-rich Highveld coal

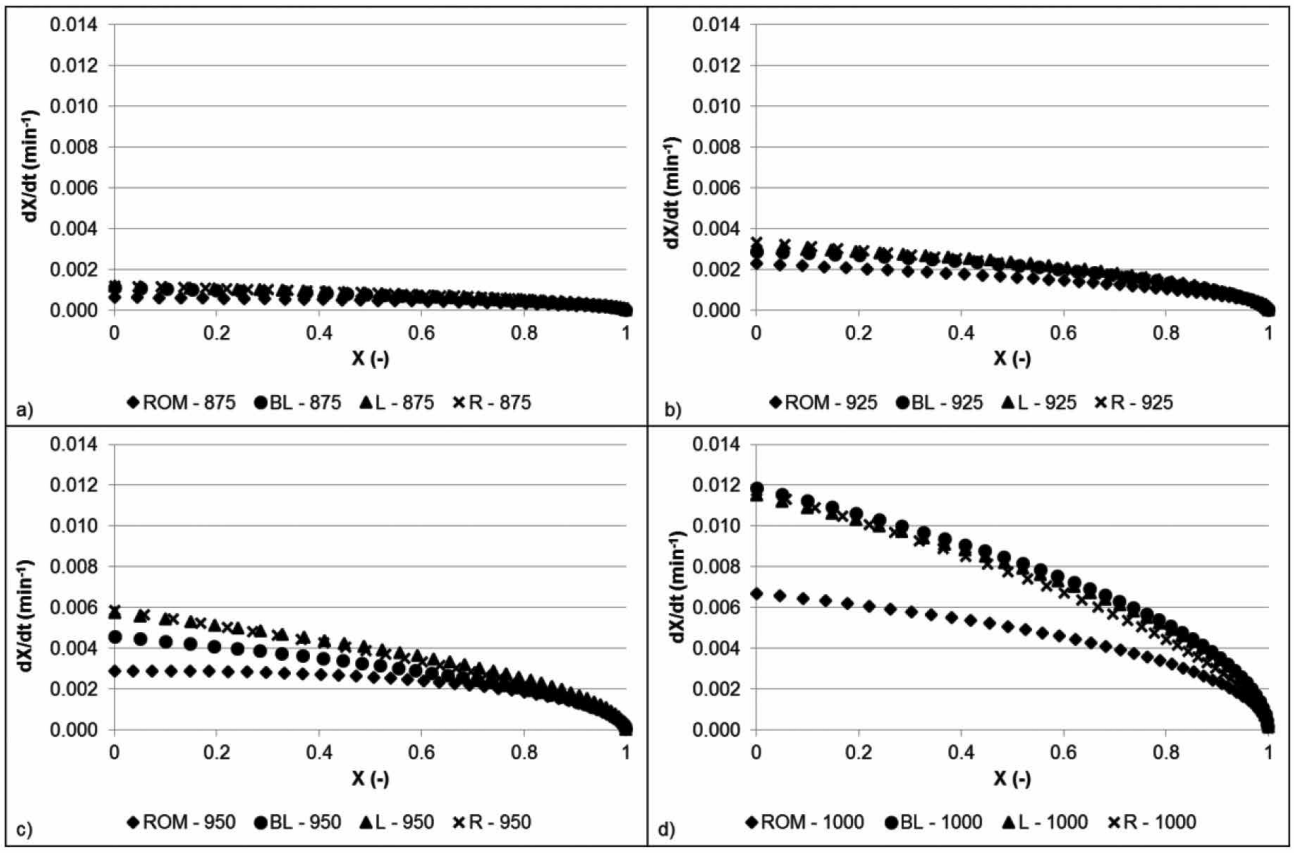

Figure 4—Conversion rate comparisons between ROM coal char, BL, L, and R charred briquettes at temperatures between 875 and 1000°C

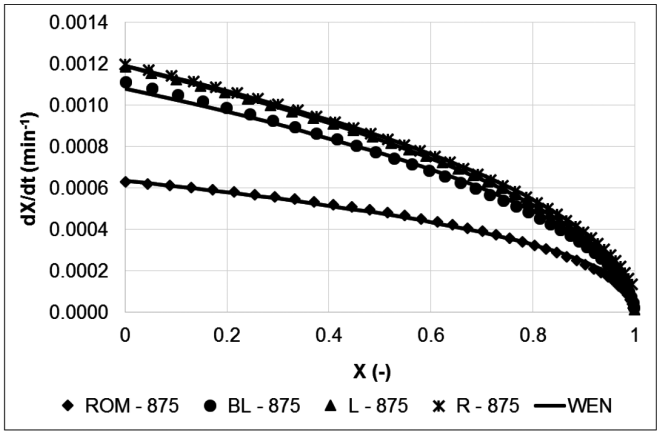

Figure 5—Wen model prediction for ROM coal, BL, L, and R briquette char reactivity at 875°C

Table IV

Reactivity data obtained using the Wen model

T (°C)	ROM				BL				L				R			
	m	$k.10^3$ (min^{-1})	QOF (%)	t_{50} (h)	*m*	$k.10^3$ (min^{-1})	QOF (%)	t_{50} (hr)	*m*	$k.10^3$ (min^{-1})	QOF (%)	*t*50 (h)	*m*	$k.10^3$ (min^{-1})	QOF (%)	t_{50} (h)
875	0.41	0.64	90	15	0.49	1.08	94	9	0.51	1.19	96	8	0.49	1.19	98	8
900	0.29	1.19	77	8	0.45	2.08	92	5	0.42	2.13	96	4	0.48	2.09	97	5
925	0.48	2.27	97	4	0.49	3.03	89	3	0.50	3.23	88	3	0.56	3.33	98	3
950	0.36	3.18	86	3	0.51	4.61	97	2	0.51	5.76	95	2	0.60	5.84	98	2
1000	0.46	6.83	93	1	0.51	11.88	97	1	0.51	11.54	97	1	0.60	11.67	98	1

for the manufactured briquettes. Also presented in Table IV is the time required to reach 50% conversion for the ROM coal and briquetted chars. On average, the briquetted coal chars reached 50% conversion 1.6 times faster than the ROM coal chars, which is verified by the increased micropore surface area and porosity (indicated in Figure 2).

The reactivity constants obtained from the Wen model were used in the construction of Arrhenius plots (Figure 6) to further study the effect of the gasification reaction temperature. A linear fit was observed for the results obtained for all four formulations, indicating that the gasification reactions follow Arrhenius-type kinetics (Dutta, Wen, and Belt, 1977; Guizani, Sanz, and Salvador, 2013). Activation energy values were found to range between 222 and 229 kJ/mole, as seen in Table V. These values are within the range observed by Everson *et al.* (2013) during CO_2 gasification of an inertinite-rich Highveld coal.

Conclusion

The industrial use of fine coal discards carries both economic and environmental benefits for coal-dependent countries such as South Africa. In this study, the reactivity of briquettes derived from fine discard coal was evaluated for application in FBDB gasification. The briquetting process itself brought significant changes to the char reactivity compared to ROM coal char. The manufactured briquetted chars exhibited approximately double the gasification reaction rate of the ROM coal and can therefore directly be used in the current FBDB gasification process. Analysis of the CO_2 gas adsorption data showed that briquetted chars had similar micropore surface areas, which were considerably higher than that of the ROM coal char. The agglomeration of coal fines was found to enhance the CO_2 gasification reaction rate as a result of compaction differences between the briquette and ROM coal chars. The binders brought about no substantial changes to the char reactivities, due to the extensive heat the briquettes were subjected to during the devolatilization and gasification processes – resulting in the disintegration of the binders. Upon investigating various kinetic models, the Wen model was found to predict the reactivity data closely. No significant differences in the activation energy values of the ROM coal and manufactured briquettes were observed. The mechanical and thermal analyses of the lignosulphonate- and resin-bound briquettes showed promising results for industrial application, meriting a techno-economic study to determine economic applicability.

Table V

Activation energies of ROM,BL, L, and R briquette chars

	ROM	BL	L	R
E_a (kJ/mole)	229	227	222	224

Acknowledgements

The information presented in this paper is based on research financially supported by the South African Research Chairs Initiative (SARChI) of the Department of Science and Technology and National Research Foundation of South Africa (Coal Research Chair Grant No. 86880).

Any opinion, finding, or conclusion or recommendation expressed in this material is that of the author(s) and the NRF does not accept any liability in this regard.

Nomenclature

a	Polynomial coefficient (dimensionless)
AI	Alkali Index
d_{80}	Screen diameter at which 80% cumulative mass is retained (µm)
E_a	Activation energy (kJ/mole)
k	Reactivity constant (min^{-1})
m	Reaction order (dimensionless)
m_{ash}	Mass of sample ash (g)
m_i	Initial sample mass (g)
m_t	Sample mass at time t (g)
t_{50}	Time at 50% conversion
X	Conversion (dimensionless)
dX/dt	Conversion rate (min^{-1})

References

Bell, F.G., Bullock, S.E.T., Hälbich, T.F.J., and Lindsay, P. 2001. Environmental impacts associated with an abandoned mine in the Witbank Coalfield, South Africa. *International Journal of Coal Geology*, vol. 45, no. 2-3. pp.195-216.

Brebu, M., Cazacu, G., and Chirila, O. 2011. Pyrolysis of lignin - a potential method for obtaining chemicals and/or fuels. *Cellulose Chemistry and Technology*, vol. 45, no. 1. pp. 43–50.

Bunt, J.R., Neomagus, H.W.J.P., Botha, A., and Waanders, F.B. 2015. Reactivity study of fine discard coal agglomerates. *Journal of Analytical and Applied Pyrolysis*, vol. 113. pp. 723–728.

Bunt, J.R. and Waanders, F.B. 2008. An understanding of lump coal physical property behaviour (density and particle size effects) impacting on a commercial-scale Sasol-Lurgi FBDB gasifier. *Fuel*, vol. 87, no. 13-14. pp. 2856–2865.

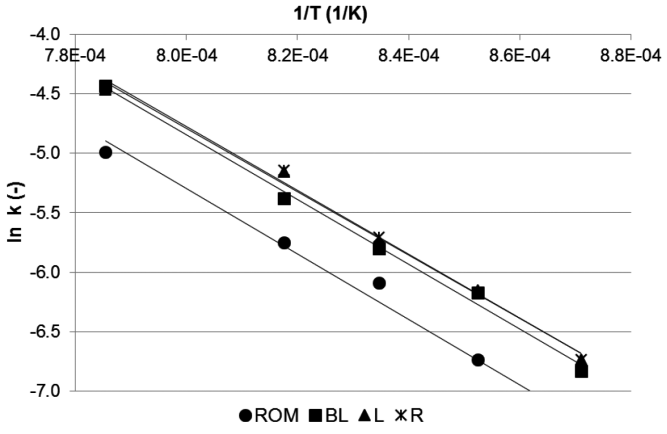

Figure 6—ROM, BL, L, and R Arrhenius plots

Cai, H.Y., Güell, A.J., Chatzakis, I.N., Lim, J.Y., Dugwell, D.R., and Kandiyoti, D.R. 1996. Combustion reactivity and morphological change in coal chars: effect of pyrolysis temperature, heating rate and pressure. *Fuel*, vol. 75, no. 1. pp. 15–24.

Coetzee, S., Neomagus, H.W.J.P., Bunt, J.R., and Everson, R.C. 2013. Improved reactivity of large coal particles by K_2CO_3 addition during steam gasification. *Fuel Processing Technology*, vol. 114. pp. 75–80.

Coetzee, S., Neomagus, H.W.J.P., Bunt, J.R., Strydom, C.A. and Schobert, H.H. 2014. The transient swelling behaviour of large (-20 + 16 mm) South African coal particles during low-temperature devolatilisation. *Fuel*, vol. 136. pp. 79–88.

Department of Energy. 2016. Basic Electricity. http://www.energy.gov.za/files/electricity [accessed 17 March 2016].

Dutta, S., Wen, C.Y., and Belt, R.J. 1977. Reactivity of coal and char. 1. In carbon dioxide atmosphere. *Industrial and Engineering Chemistry Process Design and Development*, vol. 16, no. 1. pp. 20–30.

England, T. 2000. The economic agglomeration of fine coal for industrial and commercial use. Coaltech, Johannesburg.

Everson, R.C., Okolo, G.N., Neomagus, H.W.J.P. and Dos Santos, J.M. 2013. X-ray diffraction parameters and reaction rate modeling for gasification and combustion of chars derived from inertinite-rich coals. *Fuel*, vol. 109. pp.148–156.

Guizani, C., Sanz, F.J.E., and Salvador, S. 2013. The gasification reactivity of high-heating-rate chars in single and mixed atmospheres of H_2O and CO_2. *Fuel*, vol. 108. pp. 812–823.

Huang, H., Wang, K., Bodily, D.M., and Hucka, V.J. 1995. Density measurements of Argonne Premium coal samples. *Energy and Fuels*, vol. 9, no. 1. pp. 20–24.

Irfan, M.F., Usman, M.R., and Kusakabe, K. 2011. Coal gasification in CO_2 atmosphere and its kinetics since 1948: A brief review. *Energy*, vol. 36, no. 1. pp. 12–40.

Jeffrey, L.S. 2005. Characterization of the coal resources of South Africa. *Journal of the South African Institute of Mining and Metallurgy*, vol. 105, no. 2. pp. 95–102.

Kotsiopoulos, A. and Harrison, S.T.L. 2017. Application of fine desulfurised coal tailings as neutralising barriers in the prevention of acid rock drainage. *Hydrometallurgy*, vol. 168. pp. 159–166.

Kucherenko, V.A., Shendrik, T.G., Tamarkina, Y.V.. and Mysyk, R.D. 2010. Nanoporosity development in the thermal-shock KOH activation of brown coal. *Carbon*, vol. 48, no. 15. pp. 4556–4577.

Laurendeau, N.M. 1978. Heterogeneous kinetics of coal char gasification and combustion. *Progress in Energy and Combustion Science*, vol. 4, no. 4. pp. 221–270.

Leokaoke, N.T., Bunt, J.R., Neomagus, H.W.J.P., Strydom, C.A. and Mthombo, T.S. 2018. Manufacturing and testing of briquettes from inertinite-rich low grade coal fines using various binders. *Journal of the Southern African Institute of Mining and Metallurgy*, vol. 118, no. 1. pp. 83–88.

Liu, G., Benyon, P., Benfell, K.E., Bryant, G.W., Tate, A.G., Boyd, R.K., Harris, D.J., and Wall, T.F. 2000. The porous structure of bituminous coal chars and its influence on combustion and gasification under chemically controlled conditions. *Fuel*, vol. 79, no. 6. pp. 617–626.

Liu, L., Cao, Y., and Liu, Q. 2015. Kinetics studies and structure characteristics of coal char under pressurized CO_2 gasification conditions. *Fuel*, vol. 146. pp. 103–110.

Lu, L., Kong, C., Sahajwalla, V., and Harris, D. 2002. Char structuralm ordering during pyrolysis and combustion and its influence on char reactivity. *Fuel*, vol. 81, no. 9. pp. 1215–1225.

Mahinpey, N. and Gomez, A. 2016. Review of gasification fundamentals and new findings: Reactors, feedstock, and kinetic studies. *Chemical Engineering Science*, vol. 148. pp. 14–31.

Mangena, S.J. and de Korte, G.J. 2004. Development of a process for producing low-smoke fuels from coal discards. Division of Mining Technology, CSIR, Pretoria.

Mangena, S.J., de Korte, G.J., McCrindle, R.I., and Morgan, D.L. 2004. The amenability of some Witbank bituminous ultra fine coals to binderless briquetting. *Fuel Processing Technology*, vol. 85, no. 15. pp. 1647–1662.

Mangena, S.J. and du Cann, V.M. 2007. Binderless briquetting of some selected South African prime coking, blend coking and weathered bituminous coals and the effect of coal properties on binderless briquetting. *International Journal of Coal Geology*, vol. 71, no. 2. pp. 303–312.

Massaro, M.M., Son, S.F., and Groven, L.J. 2014. Mechanical, pyrolysis, and combustion characterization of briquetted coal fines with municipal solid waste plastic (MSW) binders. *Fuel*, vol. 115. pp. 62–69.

Matjie, R.H., French, D., Ward, C.R., Pistorius, P.C. and Li, Z. 2011. Behaviour of coal mineral matter in sintering and slagging of ash during the gasification process. *Fuel Processing Technology*, vol. 92, no.8. pp.1426–1433.

Mishra, S.L., Sharma, S.K. and Agarwal, R. 2000. Briquetting of lignite for domestic fuel. *Science and Industrial Research*, vol. 59, no. 5. pp. 413–416.

Molina, A. and Mondragon, F. 1998. Reactivity of coal gasification with steam and CO2. *Fuel*, vol. 77, no. 15. pp. 1831–1839.

Motaung, J.R., Mangena, S.J., de Korte, G.J., McCrindle, R.I., and van Heerden, J.H.P. 2007. Effect of coal composition and flotation reagents on the water resistance of binderless briquettes. *Coal Preparation*, vol. 27, no. 4. pp. 230–248.

Ochoa, J., Cassanello, M.C., Bonelli, P.R., and Cukierman, A.L. 2001. CO_2 gaification of Argentinean coal chars: a kinetic characterization. *Fuel Processing Technology*, vol. 74, no. 3. pp. 161–176.

Okolo, G.N., Everson, R.C., Neomagus, H.W.J.P., Roberts, M.J., and Sakurovs, R. 2015. Comparing the porosity and surface areas of coal as measured by gas adsorption, mercury intrusion and SAXS techniques. *Fuel*, vol. 141. pp. 93–304.

Richards, S.R. 1990. Physical testing of fuel briquettes. *Fuel Processing Technology*, vol. 25, no. 2. pp. 89–100.

Roberts, D.G. and Harris, D.J. 2007. Char gasification in mixtures of CO_2 and H_2O: Competition and inhibition. *Fuel*, vol. 86, no. 17. pp. 2672–2678.

Rosin, A., Schröder, H.W., and Repke, J.U. 2014. Briquetting press as lock-free continuous feeding system for pressurized gasifiers. *Fuel*, vol. 116. pp. 871–878.

Rubio, B., Izquierdo, M.T., and Segura, E. 1999. Effect of binder addition om the mechanical and physicochemical properties of low rank coal char briquettes. *Carbon*, vol. 37, no. 11. pp. 1833–1841.

Sakawa, M., Sakurai, Y. and Hara, Y. 1982. Influence of coal characteristics on CO_2 gasification. Fuel, vol. 61, no. 8. pp. 717–720.

Spath, P.L. and Dayton, D.C. 2003. Preliminary screening - technical and economic assessment of synthesis gas to fuels and chemicals with emphasis on the potential for biomass-derived syngas. Report NREL/TP-510-34929). National Renewable Energy Laboratory, Golden CO.

Tarasov, D., Shahi, C., and Leitch, M. 2013. Effect of additives on wood pellet physical and thermal characteristics: A review. ISRN Forestry, 2013. pp. 1–6.

Teixeira, S.R., Pena, A.F.V., and Miguel, A.G. 2010. Briquetting of charcoal from sugar-cane bagasse fly ash (scbfa) as an alternative fuel. *Waste Management*, vol. 30, no. 5. pp. 804–807.

Van Dyk, J.C., Benson, S.A., Laumb, M.L., and Waanders, B. 2009. Coal and coal ash characteristics to understand mineral transformations and slag formation. *Fuel*, vol. 88, n. 6. pp.1057–1063.

Van Dyk, J.C., Keyser, M.J., and Coertzen, M. 2006. Syngas production from South African coal sources using Sasol-Lurgi gasifiers. *Coal Geology*, vol. 65, no. 3. pp. 243–253.

Wagner, N.J. 2008. The characterization of weathered discard coals and their behaviour during combustion. *Fuel*, vol. 87, no. 8. pp. 1687–1697.

Wen, C.Y. 1968. Noncatalytic heterogeneous solid-fluid reaction models. I*ndustrial and Engineering Chemistry*, vol. 60, no. 9. pp. 34–54.

Nthabiseng T. Leokaoke carried out the study and wrote the manuscript.

John R. Bunt supervised the study and proof read the manuscript.

Hein W.J.P. Neomagus supervised the study and proof read the manuscript.

Frans B. Waanders Neomagus supervised the study and proof read the manuscript.

Christien A. Strydom proof read the manuscript. ◆